

Geodesic mode instability driven by electron and ion fluxes in tokamaks

A.G. Elfimov¹, F. Camilo de Souza¹, R.M.O. Galvão¹,

J. Krbec^{2,3}, J. Seidl², J. Stöckel², M. Hron², J. Havlicek², K. Mitošinková^{2,4}

¹*Institute of Physics, University of São Paulo, São Paulo, 05508-090, Brazil*

²*Institute of Plasma Physics AS CR, Prague, Czech Republic*

³*Faculty of Nuclear Sciences and Physical Engineering, Czech Technical University, Prague, Czech Republic;*

⁴*Faculty of Mathematics and Physics, Charles University in Prague, Prague, Czech Republic*

Geodesic Acoustic Modes (GAM) are $M=0, N=0$ axisymmetric toroidal modes combined with $M=\pm 1, \pm 2$ poloidal side-bands and driven by the electron and anisotropic ion pressure perturbations with the frequency $\omega_G^2 \approx (7T_i/2 + 2T_e)/R_0^2 m_i$. These modes may be important for plasma transport as it has been theoretically discussed^[2] and observed in experiments^[4-7]. Furthermore, they may be useful as a diagnostic tool to indicate L-H confinement transition in tokamaks^[5]. Eigenmodes in the geodesic frequency range have been experimentally detected under a wide range of conditions in various tokamaks. Typically, GAM oscillations are observed during counter NB injection^[7,8], but they may also appear in ohmic discharges^[6,8]. The nature of the experimentally observed geodesic eigenmodes is still not clear and several different mechanisms might be responsible for their dispersion and manifest themselves in different conditions. Recently, it has been theoretically shown that GAMs may be driven by an electric current with velocity along the equilibrium magnetic field in combination with the diamagnetic drift^[3]. The instability occurs only when the electron current velocity is higher than the GAM phase velocity of sidebands, $V_{e0} > Rq\omega$.

Here, we extend previous studies^[3] and investigate whether the parallel plasma flow can drive the GAMs via coupling with the ion drift dynamics or/and the parallel current. Finally, comparison with NB experiments in COMPASS tokamak is discussed.

Theoretical results

The kinetic treatment of the GAM type modes is fully performed by taking into account the parallel electron and ion dynamics and diamagnetic drifts. The standard drift kinetic equation, in the scalar potential limit for the parallel electric field, $E_3 = h_\theta E_2$, with quasi-toroidal set of coordinates (r, θ, ζ) is used in the large aspect ratio tokamak approach $R_0 \gg r$ with the circular surfaces ($R = R_0 + r \cos \theta$, $z = r \sin \theta$), which are formed by the magnetic field with toroidal and poloidal components, $B_\zeta = B_0 R_0 / R$, $B_\theta = r B_\zeta / q R_0$

$$\frac{\partial f}{\partial \vartheta} - \frac{i\Omega f}{w} = \frac{eF}{mw} \left[\frac{(w - v_{_0})E_3}{k_0 v_T^2} + \frac{2 + \eta(w^2 + u^2 - 3)}{2k_0 v_T \omega_c d_r} E_2 - \frac{(2w^2 + u^2)}{2v_T \omega_c k_0 R} E_1 \sin \vartheta \right]. \quad (1)$$

Here, $\Omega = \omega/k_0 v_T$ and $\omega_c = eB/mc$ are the normalized wave and cyclotron frequencies, E_i are components of wave field, $k_0 = h_g/r = 1/qR$ is the parallel wave vector, $h_g = B_g/B_0$ is magnetic field inclination, $w = v_{||}/v_T$ and $u = v_{\perp}/v_T$ are the normalized space velocities $v_{Te,i} = \sqrt{T_{e,i}/m_{e,i}}$ are electron and ion thermal velocities, and $\partial n_0/\partial r = -n_0/d_r$ is density gradient, $\eta_{e,i} = \partial \ln T_{e,i}/\partial \ln n_0$. A shifted Maxwell distribution $F_{i,e} = F_M|_{w=w-v_0}$ by the parallel velocity $V_{i,e0}$, is assumed for ions and the electrons. For adiabatic electrons $\sqrt{\varepsilon}v_{Te}/qR \gg \omega$ and $1 \gg (V_{e0}/v_{Te})^2$, the electron density perturbations \tilde{n}_e via $E_3 = E_s \sin \vartheta + E_c \cos \vartheta$ are

$$n_{es} = (e_i n_0 R_0 q / T_e) \left[\sqrt{\pi \mu / 2\tau_e} v_{e0} E_s - E_c \right], \quad n_{ec} = (e_i n_0 R_0 q / T_e) \left[\sqrt{\pi \mu / 2\tau_e} v_{e0} E_c + E_s \right] \quad (2)$$

where $\mu = m_e/m_i$, $v_{e0} = V_{e0}/v_{Ti}$, $\tilde{n}_e = n_{es} \sin \vartheta + n_{ec} \cos \vartheta$, $\tau_e = T_e/T_i$. Using fluid limit, $\omega R_0/v_{Ti} \gg 1/q$ and $k_r^2 \rho_i^2 \ll 1$, the solution of Eq.(1) for ions is found, then, it is integrated in velocity space to obtain density perturbations. Further, using the quasi-neutrality condition with the electron density (2), one finds the parallel electric field components in the form

$$E_s = -4 \frac{v_{i0} \tau_e v_{Ti} E_1}{\omega_{ci} R_0 D_s} + \frac{i E_c}{2 D_s} \left[\sqrt{2\pi} i \sqrt{\frac{\mu}{\tau_e}} v_{e0} \Omega^2 + \tau_e (\Omega^2 + 1 + \eta_i) \frac{\rho}{\Omega} + 2 \frac{v_{i0} \tau_e}{\Omega} \right]; \quad (3a)$$

$$E_c = \frac{\tau_e v_{Ti}}{\omega_{ci} R_0 D_c} \left\{ \sqrt{2\pi} \left[\frac{D_s}{2} \Omega^2 (\Omega^2 + 1) \exp\left(-\frac{\Omega^2}{2}\right) - 2 \sqrt{\frac{\mu}{\tau_e}} v_{i0} v_{e0} \Omega^2 \right] + i \left[2(\Omega^2 + 2) D_s / \Omega + (8\tau_e + D_s \Omega^2 + 7D_s) v_{i0}^2 / \Omega + 4\tau_e \rho (\Omega^2 + 1 + \eta_i) v_{i0} / \Omega \right] \right\} \quad (3b)$$

$$\text{where } D_s = \Omega^2 - \tau_e \left[1 + (1 + \eta_i) \rho v_{i0} + \sqrt{\pi/2} i \Omega \exp(-\Omega^2/2) \right] \quad (4)$$

$$D_c = D_s^2 - \left[\tau_e (\Omega^2 + 1 + \eta_i) \rho / \Omega + 2 v_{i0} \tau_e / \Omega + i \sqrt{\pi \mu / 2\tau_e} (v_{e0} + \tau_e \rho (1 - \eta_e/2)) \Omega^2 \right]^2.$$

Using the electric fields (3) in the averaged sum of the radial electron and ion currents together with the ion radial polarization current in the GAM resonance condition

$$\langle \tilde{j}_r^e + \tilde{j}_r^i \rangle + j_p = 0, \text{ where } j_p = -i\omega c^2 E_1 / 4\pi c_A^2, \quad c_A = B / \sqrt{4\pi n_i m_i},$$

is the ion polarization current, we get the equation for the GAM continuum frequency

$$\frac{\Omega_G^2}{q^2} = \left(\frac{\omega_G^2 R_0^2}{v_{Ti}^2} \right) \approx \left[\frac{7}{2} + 2\tau_e + (4 + 2\tau_e) \left(\frac{V_{i0}}{v_{Ti}} \right)^2 + \frac{23 + 59(V_{i0}/v_{Ti})^2 + 4\tau_e(4 + \tau_e)}{q^2(7 + 4\tau_e)} \right] \quad (5)$$

From imaginary part of Eq.(5), we obtain the threshold of the GAM instability

$$\gamma \approx \sqrt{\frac{\pi}{2}} \frac{v_{Ti} \tau_e q}{2 R_0 \Omega_G^2} \left[\frac{\rho_{Li} V_{e0}}{d_r h_g v_{Te}} (2 + 2\eta_i + 3\tau_e) + 4 \frac{V_{i0} V_{e0}}{v_{Ti} v_{Te}} - 0.03 \exp(2 - q^2/2) \right] \quad (6)$$

GAM observation during NB heating in COMPASS tokamak

COMPASS ($R = 0.56$ m, $a = 0.2$ m) is a tokamak with ITER-like shape diverted plasma configuration. The diagnostics was supplied by magnetic coils ^[8] for measurement of poloidal and radial magnetic field fluctuations with 2 MHz sampling rate, using two poloidal rings of Mirnov coils and a set of saddle loops covering the whole toroidal angle. There are two pneumatic reciprocating probe manipulators ^[8], which are equipped by combination of Langmuir probes measuring floating potential V_{fl} and/or ion saturation current I_{sat} , and ball-pen probes providing fast measurement of a plasma potential, as well the electron temperature together with two high resolution Thomson scattering systems for core and for edge plasmas. GAM like oscillations ($N=0$, $M=0-3$) in the frequency band $f=30-37$ kHz were detected by the magnetic and Langmuir probes ^[8] with high coherence level (at the position $\Delta r \approx -1-2$ cm deep from the last magnetic surface) during ohmic discharges shown in Fig.1 in deuterium plasmas ($B_i=1.15$ T, $I_p=180$ kA, elongation $\kappa=1.8$, $n_0=4-5 \cdot 10^{19}$ m⁻³, $T_{e0}=800-900$ eV). This GAM frequency corresponds to theoretically predicted one ^[1, 3] assuming the ion temperature $T_{ia} \approx T_{ea} = 30-35$ eV at the border shown in Eq.(5). Series of discharges with co (similar to #11035, 12 A, $U_{NB}=40$ keV, $P_{NB}=360$ kW) and counter NB injection (#11502, 12A, $U_{NB}=40$ keV, $P_{NBI} \sim 370$ kW) is used to study NB heating effect on GAMs presented in Fig.2. With NB application, it is observed that the GAM frequency increases $\Delta f \approx 20\%$ for co and $\Delta f \approx 16\%$ for counter injection. Dramatic changes in the GAM amplitude occur during the NB injection period $t_{NB}=1090-1170$ ms. While the GAM amplitude increases moderately during the counter injection, the GAM instability is strongly suppressed by the co-injection, as it is shown in Fig.2, possibly, due rotation. Here, we note that there is no phase resonance between the beam circulation and GAM frequency $V_{NB} = \sqrt{2U_{NB}/m_i} \gg R_0 q \omega_G$.

Discussion

The frequency increase with NB application may be partly attributed to estimates of the electron/ion temperature variation, which is not enough to explain the GAM frequency increasing that needs to have $\Delta T_e + \Delta T_i \approx 35-40\%$. Here, we propose that part of the variation may be attributed to plasma rotation induced by NB that should be $V_{i0}/v_{\pi} \approx 0.4$ according to Eq.(5). To explain the GAM amplitude variation, we assume that it should be proportional to the instability increment in Eq.(6). In the ohmic stage, the instability may be driven by the cross term between the electron velocity and ion drift corresponding to the first term in Eq(6). A condition for the instability, large electron current speed $V_{e0} \gg Rq\omega_G > V_{i0}$, is satisfied for the entire tokamak cross-sections, calculating the current profile with EFIT code. For counter injection, the electron and ion velocities have the same direction and their cross term might

increase the instability, whereas this term may strongly reduce it for co-injection, when rotation velocity is larger than drift velocity $V_{i0} > \rho_{Li} v_{Ti} / d_r h_g$.

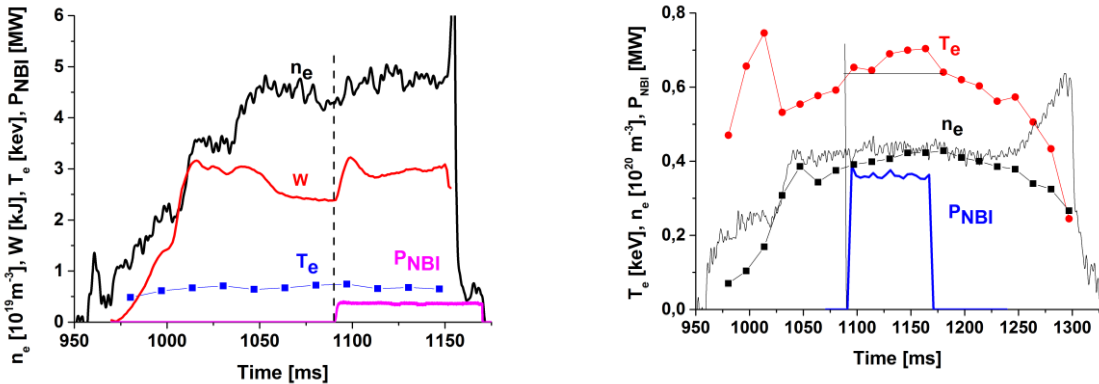


Fig.1. Temporal evolution of electron temperature, line density and energy during counter (#11502, left) and co NB injection without energy (#11035, right).

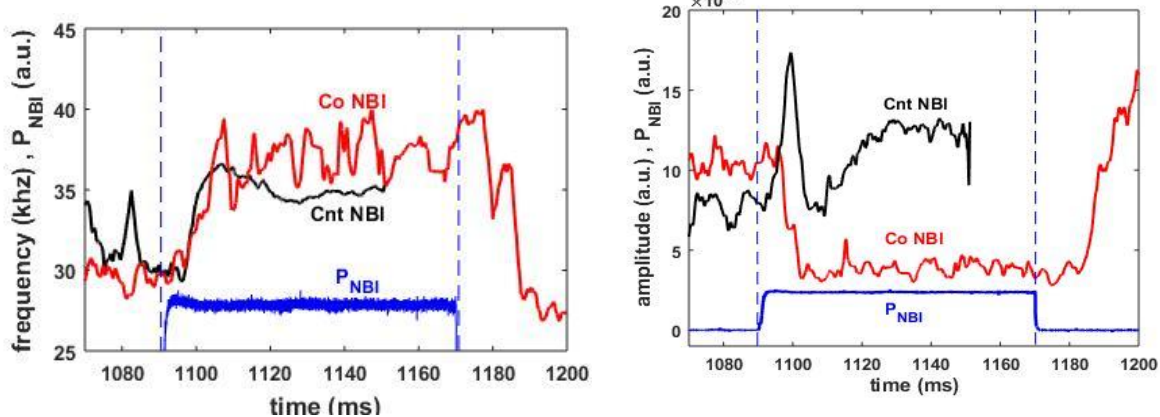


Fig.1. Temporal evolution of frequency and amplitude of magnetic signals during counter and co NB injection.

Finally, we conclude that the theoretically found GAM instability, which is increased or suppressed by plasma ion flux, may indeed be driven by the NB injection as observed in COMPASS experiments.

Acknowledgements. The theoretical part of work was supported by FAPESP (Research Foundation of the State of São Paulo), contract 2011/50773-0, Brazil and the COMPASS experiments were supported by Czech Science Foundation grant GA16-25074S and GA14-35260S and co-funded by MEYS projects number 8D15001 and LM2015045.

- [1] F. Zonca and L. Chen, R.A. Santoro *Plas. Phys. & Contr. Fusion* **38**, 2011 (1996).
- [2] P. H. Diamond *et al* (2005), *Plasma Phys. Controlled Fusion*, **47**, R35.
- [3] A. G. El'fimov, R. M. O. Galvão, A. I. Smolyakov (2014) *Phys. Let-A* **378**, 800.
- [4] G. R. McKee *et al* (2006) *Plasma Phys. Controlled Fusion*, **48**, S123.
- [5] G.D. Conway *et al* (2011) *PRL*, **106**, 065001.
- [6] A.V. Melnikov *et al* (2006) *Plasma Phys. & Control. Fusion*, **48** S87.
- [7] G. Matsunaga *et al* 39th EPS Conference & 16thICPP, P2.062, July 2012, Stockholm/Sweden.
- [8] J. Seidl *et al* 42nd EPS Conference on Plasma Physics, P4.103, June 2015, Lisbon, Portugal.